Biological activity of laminin/polylaminin-coated poly-ℇ-caprolactone filaments on the regeneration and tissue replacement of the rat sciatic nerve

R. de Siqueira-Santos [a,d], G. Sardella-Silva [a,b], M.A. Nascimento [c], L. Teixeira de Oliveira [d], T. Coelho-Sampaio [c], V.T. Ribeiro-Resende [a,b,*]

[a] Universidade Federal do Rio de Janeiro, Instituto de Biofísica Carlos Chagas Filho, Laboratório de Neuroquímica, Centro de Ciências da Saúde Bl. C, Cidade Universitária, 21949-900 Rio de Janeiro, RJ, Brazil
[b] Universidade Federal do Rio de Janeiro, Núcleo Multidisciplinar de Pesquisa em Biologia - Numpex-Bio, Campus Duque de Caxias, Estrada de Xerém, No. 27, 25245-390 Duque de Caxias, RJ, Brazil
[c] Universidade Federal do Rio de Janeiro, Instituto de Ciências Biomédicas, Laboratório de Biologia da Matriz Extracelular, Centro de Ciências da Saúde Bl. A, Cidade Universitária, 21949-900 Rio de Janeiro, RJ, Brazil
[d] Universidade Federal do Rio de Janeiro, Instituto de Bioquímica Médica Leopoldo de Meis, Laboratório de Agregação de Proteínas e Amiloidoses, Centro de Ciências da Saúde, Bl. E, Cidade Universitária, 21949-900 Rio de Janeiro, RJ, Brazil

ARTICLE INFO

ABSTRACT

Unlike the central nervous system, peripheral nerves can regenerate after injury. However, depending on the size of the lesion, the endogenous regenerative potential is not enough to replace the lost nerve tissue. Many strategies have been used to generate biomaterials capable of restoring nerve functions. Here, we set out to investigate whether adsorbing the extracellular matrix protein, laminin (LM), to poly-ℇ-caprolactone (PCL) filaments would enhance functional nerve regeneration. Initial in vitro studies showed that explants of dorsal root ganglia (DRGs) of P1 neonate mice exhibited stronger neuritogenesis on a substrate of LM that had been previously polymerized (polylaminin [polyLM]) than on ordinary LM. On the other hand, when silicone tubes filled with PCL filaments were used to bridge a 10-mm sciatic nerve gap in rats, only filaments coated with LM improved tissue replacement beyond that obtained with empty tubes. Motor function recovery correlated with tissue replacement as only LM-coated filaments consistently improved motor skills. Finally, analysis of the lateral gastrocnemius muscle revealed that the LM group presented twice the amount of α-bungarotixin–labeled motor plates. In conclusion, although polyLM was more effective in stimulating growth of sensory fibers out of DRGs in vitro, LM adsorbed to PCL filaments exhibited the best regenerative properties in inducing functional motor recovery after peripheral injury in vivo.

1. Introduction

Peripheral nerves have an intrinsic potential to regenerate after lesion; however, when damage involves extensive tissue loss, reconnection between proximal and distal stumps does not occur [1]. After axonal injury, Wallerian degeneration (WD) is triggered, initially to remove axonal and myelin debris, which is followed by proliferation of Schwann cells (SCs), recruitment of immune cells, and finally SC organization to form bands of Büngner. These structures are well described to support axonal regeneration [2–5]. During WD, activated fibroblasts of nerve connective tissue and SCs forming bands of Büngner provide significant amount of laminin (LM), helping to build a new basal lamina for nerve regeneration [6–8].

LMs are multifunctional extracellular matrix (ECM) proteins essential in embryogenesis and tissue development. They form an organized protein network that supports key processes during the development and regeneration of the nervous system, such as cell adhesion, migration, differentiation, and axonal and dendrite growth [6,9–12]. Moreover, on binding to their specific receptors (e.g. integrins or dystroglycan), LMs can induce positive cellular effects during regeneration, triggering mitogen activated protein kinase (MAP Kinase) and PI3 kinase/AKT/mTor to modulate cell survival, apoptosis, differentiation, and cell adhesion [13–15]. Laminin-211, containing three subunits, α2, β1, and γ1, is the most prominent LM type in the basal lamina of peripheral

---

nerves, where it binds to the integrin α7β1 on SCs. As a consequence, focal adhesion kinase (FAK) is attracted to integrin dimers, activating the kinase domain and phosphorylating downstream elements [16]. In vitro, this can stabilize cells such as SCs on the ECM surface, generating focal adhesion points or promoting cell migration, depending on the combination with soluble factors [16,17]. The expression of genes regulating SC survival, proliferation, and migration depends on this mechanism.

LMs are known to form planar sheet-like polymers in natural basement membranes [18]. Although the native polymeric array is lost upon LM extraction from biological tissues, it can be reestablished in a cell-free system either at an extremely high protein concentration [19] or on pH acidification [20]. Acid-induced LM polymers, termed polylaminin (polyLM), but not non-polymerized LM, have been shown to restore migration and neurite outgrowth capacities in neurons isolated from the postnatal rat brain cortex or retina [21,22] and to promote axonal growth and functional recovery after spinal cord injury [23]. The fact that polyLM exhibits a distinguished ability to stimulate neurons of the central nervous system prompted us to investigate whether it would also modulate peripheral axonal growth and nerve tissue replacement.

Over the last ten years, single or combined strategies were designed for nerve tissue replacement. Materials such as biological grafts, organic and inorganic polymers have been used with cells (e.g. Schwann or mesenchymal stem cells) and/or biologically active molecules. poly-ε-caprolactone (PCL) is one of the best studied biodegradable materials and has already been approved as a nerve scaffold by the US food and drug administration [24,25]. PCL's short-term resistance to degradation, low melting point, and specific elastic characteristics are useful properties for the regeneration of extensive nerve tissue [26–28]. In addition to these favorable characteristics, PCL microstructured filaments have been found to stimulate the formation of bands of Büngner [29].

The ultimate goal of the present work was to combine the potential benefits of microstructured PCL filaments with those of LM to describe an effective conduit for stimulating nerve regeneration. We first compared the neuritogenic properties of LM and polyLM, using dorsal root ganglion (DRG) explants, which extend both central and peripheral axons *in vivo*. Then, we coated PCL filaments with either LM or polyLM and compared their potentials to stimulate neurite outgrowth out of DRG explants with that of bare filaments. Finally, we moved to an *in vivo* model of nerve injury, in which a 10-mm segment of the sciatic nerve is removed and the two stumps are connected by a silicone tube. In this setting, we aimed to compare, morphological and functionally, the degrees of regeneration that would be obtained in four different experimental conditions, namely, (1) empty tube, (2) tube filled with uncoated filaments, (3) tube filled with LM-coated filaments, and (4) tube filled with polyLM-coated filaments. Our findings confirmed polyLM as a better substrate than LM for inducing neuritogenesis under culture conditions. Nevertheless, we unexpectedly observed that in the particular environment of a peripheral nerve *in vivo*, tubes filled with LM-coated PCL filaments revealed the best conduit for sciatic nerve regeneration.

2. Methods

2.1. Animals

All experiments were performed following the National Institutes of Health Guidelines for the Care and Use of Laboratory Animals and approved by the Ethics Committee for the Use of Animals in Research from the Federal University of Rio de Janeiro (CEUA IBCCF protocol #158 for mice C57-Black 6 and #092/16 for Wistar rats). Neonatal C57-Black 6 mice (postnatal age between P0 and P3) were used in *in vitro* experiments. For *in vivo* experiments, female Wistar rats weighing between 200 and 250 g were used. All animals were kept for the whole duration of the experiments at 12-h light/dark cycles with free access to food and water in an isolated animal room.

2.2. PCL filaments

The PCL filaments used in this study were kindly donated by Prof. Dr. Burkhard Schlosshauer of the Natural and Medical Sciences Institute associated with the University of Tübingen, in collaboration with the Institute of Textile Technology and Process Engineering, Denkendorf, Germany. Synthetic absorbable filaments were made from PCL with a molecular weight of 50,000 g/mol (Dow Tone, P767). Long microstructured filaments were formed by a technique of melting and extrusion in a spinneret at 205 °C, using a six-leaf nozzle with 24 capillaries. The yield volume was approximately 0.4 mL/min for each capillary, and the output speed was 1000 mm/min. In this state, the diameter of each capillary was 22 μm, with 66 μm of functional circumference. The bundles of filaments were washed with distilled water and wrapped around a microscope slide to facilitate handling, and the ends were sealed. Small 2-cm segments (width of a microscope slide) containing hundreds of filaments sealed at the ends were sterilized in 70% ethanol and dried [29]. Ultrastructural analysis was carried out by bonding the specimens in brackets covered with a double-sided tape and imaging in a scanning electron microscope (Jeol JSM6390LV, JEOL, Peabody, MA, USA) after sputtering with a 20-nm thick gold layer. The functionalization of the filaments was performed in a three-step process. Initially, the material surface was hydrophilized using a glow discharge of O_2 plasma for three cycles of 75 s (PELCO easiGlow™; Pelco, Redding, CA, USA). Then, the filaments were coated with poly-D-lysine (50 μg/mL H_2O; Sigma-Aldrich, São Paulo, SP, Brazil).

2.3. LM coating of the coverslip and PCL filaments

Substrates were prepared on 13-mm glass coverslips or PCL filaments by incubating either poly-L-ornithine (PLO), previously polymerized LM (polyLM) or ordinary, non-polymerized, LM for 12 h at 37 °C. PLO (used as an inert control substrate) was dissolved in water to a final concentration of 50 μg/mL. polyLM and LM were produced by diluting Engelbreth Holm Swarm-derived-LM) (#23017015, laminin-111; Life Technologies®) to 50 μg/mL with 20 mM sodium acetate (pH 4) or 20 mM Tris-HCl (pH 7), respectively, both containing 1 mM $CaCl_2$ [21]. Before cell plating, wells containing the coverslips or filaments were washed three times with phosphate-buffered saline (PBS 1x pH7.4).

2.4. DRG explants

DRG explants were obtained from P0–P3 neonatal pups. Pups were cold anesthetized and quickly decapitated. DRGs were dissected and then incubated in a culture medium (DMEM F-12) containing nerve growth factor (NGF 50 ng/mL, Life Technologies) for 1 h at 37 °C and 5% CO_2 before being plated on previously coated coverslips or filaments in 24-well plates during 3 or 7 days. NGF was kept under all experimental conditions for at least 24 h, being withdrawn from non-NGF conditions after this period. At the end of the incubation time, the culture system was carefully washed and fixed with 4% paraformaldehyde for 15 min.

2.5. Western blotting

Western blots from culture lysates were performed in a denaturing lysis buffer containing 50 mM Tris, 2% SDS, 2 mM ethylenediamine tetraacetic acid (EDTA), and a protease inhibitor cocktail (Sigma-Aldrich® code no. P2714-1BTL). Samples were homogenized and centrifuged at 10,000 rpm for 5 min (10,000 G). Protein levels were assessed by immunoblotting from 25 μg of total sample protein on the sodium dodecyl sulfate polyacrilamide gel eletropho resis (SDS-PAGE, polyacrylamide 10%). After electrophoresis, proteins were transferred to nitrocellulose membranes (Bio-Rad, CA). The membranes were blocked with 5% non-fat dried milk diluted in tris-buffered saline plus tween 20 (TBST, 200 mM Tris-HCl, 1.37 M NaCl, 1% Tween 20, pH 7.6) for 1 h at room temperature, then incubated overnight at 4 °C with primary

antibodies in TBST. Primary antibodies used were as follows: anti-AKT, anti-FAK, and its phosphorylated forms (Cell Signaling®). To confirm total protein loading, we used anti-GAPDH (Sigma®). Finally, Western blots were analyzed by optical densitometry using Scion Image® software.

2.6. Sciatic nerve lesion and microsurgery for PCL filament implanting

All surgical procedures were performed under anesthesia. Right sciatic nerves were exposed at the mid-thigh level and an approximate 10-mm nerve segment was sectioned and removed. Distal and proximal stumps were reconnected and sutured inside a 14-mm silicone tube, leaving a gap of approximately 13 mm between the two stumps inside the tube. The control group (empty tube) received only 20 μL of germ-free PBS injected into the tube (n = 6). Another group had the tube filled with PCL filaments coated with PLO (PCL group, n = 6). The LM groups were implanted with PCL filaments previously coated with LM (PCL + LM) or polyLM (PCL + polyLM) (n = 8). PCL filaments were inserted into the tube using small tweezers. After the animals recovered from anesthesia, they were returned to the animal facility and kept with food and water ad libitum for 12 weeks.

2.7. Behavioral tests

The animals were subjected to functional tests on alternate days for 12 weeks to evaluate their functional recovery after lesion. Animals were acclimated for 2 weeks before the surgeries. During this period, they were trained, and their functional baseline was set as a control for future behavioral analysis.

2.7.1. Motor functional tests

The locomotion performance of the animals was assessed using the CatWalk locomotion analysis system (Noldus Information Technology, Wageningen, Netherlands). At the end of 2 weeks of training, all animals were able to make uninterrupted runs, lasting between 2 and 4 s. After surgery, the animals were evaluated once a week, for 12 weeks. Runs of each animal were recorded by the CatWalk apparatus, and the recorded data (at least two runs per animal) were analyzed using CatWalk software (version 10.0). The parameters analyzed were the following: maximum contact area, print area, and maximum intensity of the footprint of the paw. For each parameter, values for all paws were recorded, and the ratio of the ipsilateral paw to contralateral paw was calculated and compared among the different experimental groups.

2.7.2. Rotarod® test

Motor ability and coordination were evaluated using the Rotarod apparatus (Orchid Scientific, Maharashtra, India) for rats. The ability of young adult rats to keep their balance on a rotating bar at 28 rpm was tested, and the fall latency was measured in all animal groups. Once a week, the rats underwent two trials separated by a 15-min break between them.

2.8. Histology procedures

Twelve weeks after surgery, the rats were deeply anesthetized with an intraperitoneal (IP) injection (300 mL) of a cocktail containing xylasin (3.2 mg/kg; Syntec, Cotia, SP, Brazil), ketamine (62.5 mg/kg; Syntec), and acepromazine (0.625 mg/kg; Syntec) diluted in water and perfused transcardially with a 0.9% saline solution for 10 min (10 mL/min, Masterflex®; Cole-Parmer Instrument Co.), followed by 4% paraformaldehyde (20 min) and 4% paraformaldehyde + 10% sucrose solution (10 min). The sciatic nerves or gastrocnemius muscles were kept in a 30% sucrose solution in phosphate buffer for 48 h. The nerves had the epineurium removed and were photographed under a stereomicroscope (Leica S8AP0; Leica Microsystems Nussloch GmbH). After embedding in OCT mounting medium, longitudinal sections of the sciatic nerves (18

μm) or gastrocnemius muscles (30 μm) were obtained using a cryostat (Leica CM 1850' Leica Microsystems Nussloch GmbH) and mounted directly on gelatin + 0.05% chromium alum precoated slides. Slides were stored at −20 °C for immunofluorescence procedures.

2.9. Immunostaining procedures and imaging by optical microscopy

Before immunolabeling, the slides were washed 3 times for 5 min each with PBS, permeabilized with 0.3% Triton-X-100 (Sigma-Aldrich, St. Louis, MO, USA), blocked with 10% bovine serum albumin (Sigma-Aldrich) or normal goat serum (Sigma-Aldrich) for 30 min at room temperature, and finally incubated for 2 h at room temperature or overnight at 4 °C with primary antibodies. Incubation with secondary Alexa Fluor antibodies 488 or 594 (1:600; Life Technologies) was performed in a blocking solution for 2 h at room temperature; then, nuclei were stained with 4′,6-diamidino-2-phenylindole dihydrochloride (DAPI), followed by 3 washes with PBS. Samples were mounted on microscope slides with n-propyl gallate in 80% glycerol (Sigma-Aldrich Co., St. Louis, MO). For motor end plate staining, gastrocnemius slices were incubated with α-bungarotoxin conjugated with Alexa 594 (1:200, cat# b13423; Life Technologies) for 30 min. Primary antibodies used are as follows: rabbit polyclonal anti–NF-200 (1:200, cat# n-4142; Sigma-Aldrich), mouse monoclonal Tuj-1 (1:500, cat# t5076; Sigma-Aldrich), and goat polyclonal anti-ChAT (1:100, cat# ab144p; Sigma-Aldrich).

Explants of DRGs and histological sections were visualized and photographed under light microscopy of fluorescence using the Nikon Eclipse T1 confocal microscope and of or apotome system coupled to a Zeiss Imager M2.

2.10. Quantitative analysis

2.10.1. Neuritogenesis

The neurite outgrowth of DRG cultures was evaluated in eight randomly chosen regions, by measuring the average neurite length (the distance from the beginning to the end of each neurite) of all neurites and averaging them to have a single value per DRG explant. To quantify neuritogenesis areas, the area occupied by the central ganglia was subtracted from the total area occupied by ganglia plus neurites. Analyses were carried out using Image-Pro Plus software, version 6.0.0.260.

2.10.2. Regenerated axons

The regenerated portion of the sciatic nerve inside the polyethylene tube, from the control and experimental groups, was stained with TUJ-1 (axonal marker) and photographed under 40x magnification. Images were analyzed using Zen software (Zeiss, Germany) tracing 5 lines, 25 μm apart from each other, every 1 mm from the end of the proximal stump. Using these lines, nerve thickness and TUJ 1 + axons that cross each line were quantified.

2.10.3. Motor end plate evaluation

End plates were quantified by direct counting of lateral gastrocnemius muscle sections labeled with α-bungarotoxin conjugated with Alexa 555 using an apotome epifluorescence microscope for quantitative analysis on a Zeiss.

2.11. Image processing and statistical analysis

Images were processed using the ImageJ version 1.48 program (National Institutes of Health, Bethesda, MD, USA), and all data were analyzed using GraphPad Prism 5 (GraphPad Software, Inc., La Jolla, CA, USA). Statistical analyses were performed using Student's unpaired t-test, one-way analysis of variance (ANOVA) followed by Bonferroni post-test for comparison of all pairs of columns and two-way ANOVA followed by Bonferroni post-test comparing all pairs of columns. The confidence interval was 95%, and all values are expressed as ± standard error of the mean.

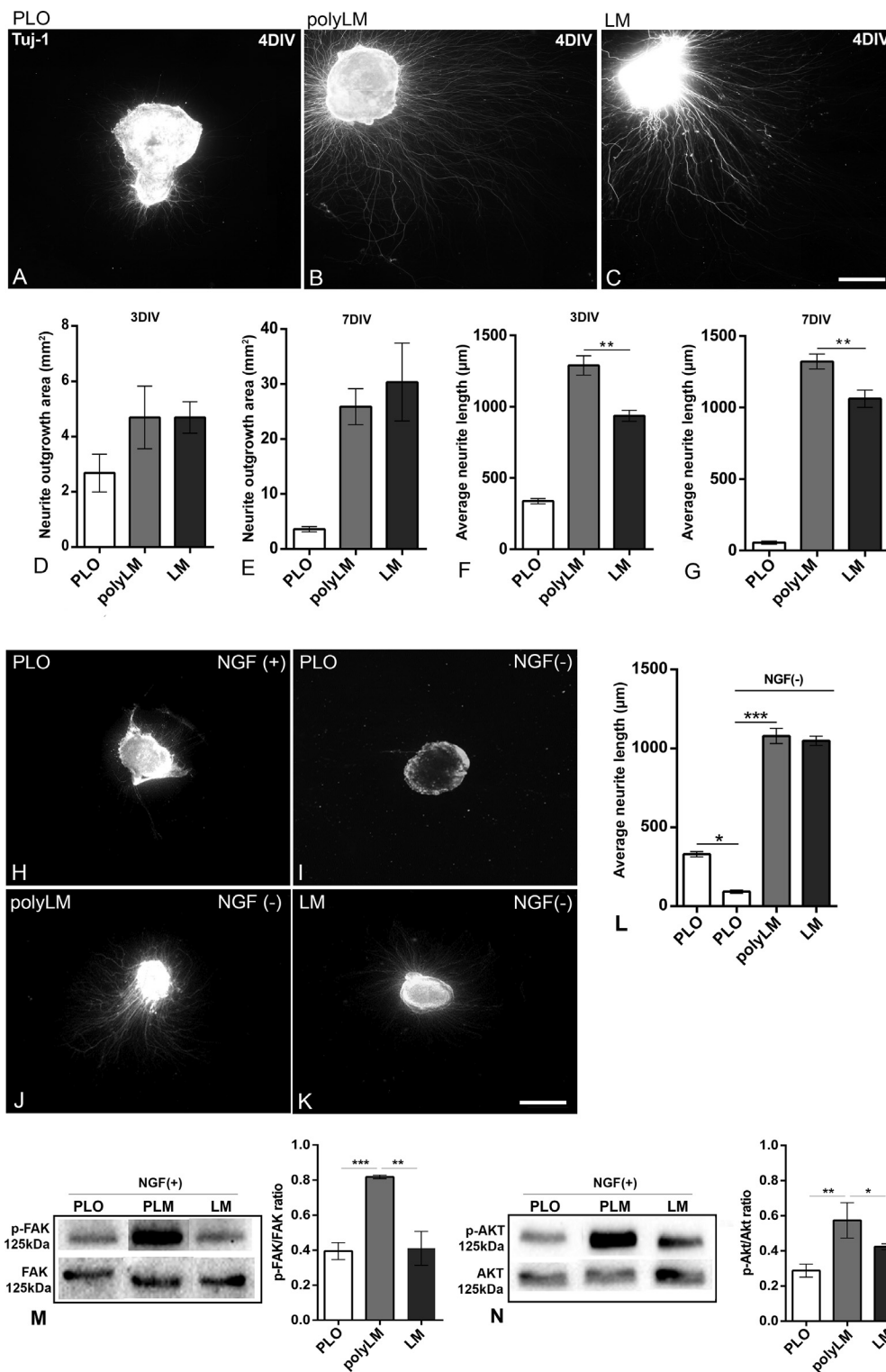**Fig. 1. Laminin substrates stimulate and support DRG neuritogenesis outgrowth *in vitro*.** (A–C) Epifluorescence images of rat P1 DRGs cultivated 4 days *in vitro* (DIV) on glass coverslips previously coated with polyornithine (A), polyLM (B), or LM substrates (C). The cytoskeleton was labeled with TUJ-1 antibody. (D–G) Quantitative analyses of neurite outgrowth area 4DIV (D) and 7DIV (E) and average neurite lengths 4DIV (F) and 7DIV (G). (H–K) Epifluorescence images of rat P1 DRG explants on polyornithine plus nerve growth factor (NGF, H) or after NGF withdrawal and cultivation for 4DIV on polyornithine (I), polyLM (J), or LM substrates (K). (L) Quantitative analysis of DRG neurite outgrowth areas after NGF deprivation. (M−N) Western blotting assay for FAK/phospho-FAK (M) or AKT/phospho-AKT (N) in explants plated for 4 days on different substrates. Activation was assessed by the ratio between phosphorylated and non-phosphorylated forms of the elements. White bars represent the polyornithine group; light and dark gray bars represent polyLM and LM groups, respectively. Scale bars: (A–C) = 100 μm; (H–K) = 500 μm. *$p < 0.01$; **$p < 0.001$; ***$p < 0.0001$ by one-way ANOVA. PLO, poly-L-ornithine; DRGs, dorsal root ganglia; LM, laminin; polyLM, polylaminin; ANOVA, analysis of variance.
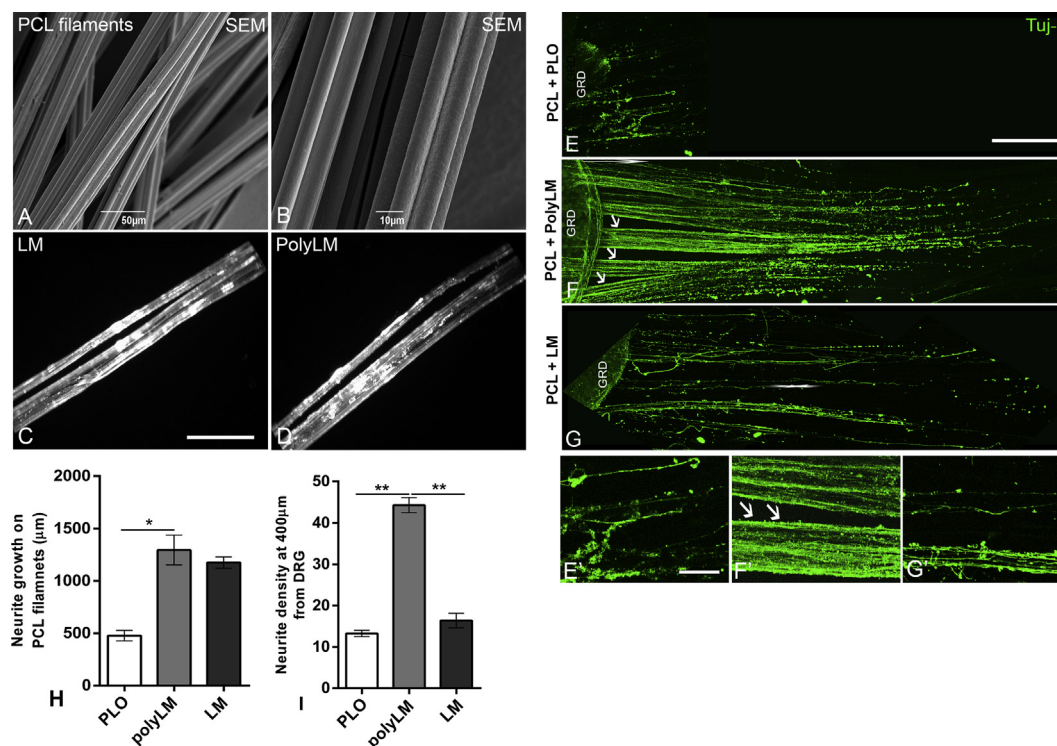
Fig. 2. Microstructured PCL filaments precoated with polyLM improve and organize neurite growth from DRG explants. (A–B) Scanning electron microscopy (SEM) images of PCL filaments evidencing the microstructure grooves in lower (A) and higher (B) magnifications. (C and D) Optical slices obtained using confocal fluorescence microscopy of filaments immunolabeled for laminin showing the protein coating of PCL filament. (E–G) Optical slices of DRG neurite outgrowth on PCL filaments coated with polyornithine (E), polyLM (F), or LM (G). (E′–G') Higher magnifications of (E)–(G). Arrows in F and F′ indicate neurites growing at the grooves of individual filaments. Neurites were immunolabeled with TUJ-1. (H) Quantitative analysis of neurite growth on PCL filaments and neurite density at 400 μm from the DRGs. Scale bars: (A) = 50 μm, (B) = 10 μm, and (C–G) = 100 μm. *$p < 0.01$; **$p < 0.001$ by one-way ANOVA. PCL, poly-ε-caprolactone; polyLM, polylaminin; LM, laminin; DRG, dorsal root ganglion; PLO, poly-L-ornithine; ANOVA, analysis of variance.; Sciatic nerve, poly-ε-caprolactone.

3. Results

3.1. polyLM provides an optimized substrate for DRG neurite outgrowth in vitro

Because LM is a well-known substrate for axonal growth and regeneration, in this first set of experiments, we investigated the ability of DRGs from P1 mice to extend neurites, in culture under the trophic activity of 20 ng/mL of NGF. Two LM substrates were provided, one obtained by adsorption of the protein diluted in a neutral buffer (LM) and another one obtained by adsorption of previously polymerized LM by dilution in acidic pH of acetate buffer (polyLM) [31]. After three days of incubation, we observed that both substrates of either polyLM or LM similarly increased the area of neuritogenesis in comparison with the control substrate of poly-ornithine (Fig. 1A–D, ANOVA, $p < 0.01$). After seven days, neuritogenesis areas were again similar between the two types of LM; however, in comparison with the control substrate, neurites spread significantly more (Fig. 1E, ANOVA, $p < 0.001$). Interestingly, when we measured the average lengths of neurites 3 and 7 days after incubation, polyLM induced longer neurites among all groups (Fig. 1F and G, ANOVA, $p < 0.001$). Next, we explored the ability of the substrates to give support for neurite outgrowth in the absence of NGF. Three days after incubation in the absence of NGF, the control group displayed far less neurites than in the presence of NGF (Fig. 1H and I and L, Mann–Whitney, $p < 0.01$). DRGs incubated on polyLM or LM in the absence of NGF revealed significantly longer neurites than those on poly-ornithine (Fig. 1 I-L, ANOVA, $p < 0.001$), but lengths were comparable with those observed on each substrate in the presence of NGF (Fig. 1F), suggesting that contact with LM compensated for the lack of the growth factor. Next, we investigated two signaling transducing elements downstream the activation of integrin receptors. The phosphorylation levels of FAK

(p-FAK) reflect the intensity of integrin activation. By Western blotting, followed by densitometry, we observed that the level of p-FAK on LM was equivalent to that obtained on PLO, but that incubation on polyLM led to a 2-fold increase in p-FAK (Fig. 1M, ANOVA, **$p < 0.001$; *$p < 0.01$). Similarly, when we analyzed the phosphorylation levels of AKT (p-AKT), an element downstream of FAK activation and related to neuronal survival and neurite outgrowth by the PI3 kinase/AKT/mTor signaling pathway, we again observed increased levels of p-AKT relative to PLO on polyLM, but not on LM (Fig. 1N, ANOVA, **$p < 0.001$; *$p < 0.01$). It is important to mention that although AKT phosphorylation increases in response to FAK activation, a basal level of p-AKT is expected to occur even in the absence of the substrates owing to the presence of NGF in the assay. This was indeed observed (Fig. 1N, left lanes). Together, the results in this section indicate that both forms of LM provide efficient substrates for neurite outgrowth even in the absence of NGF. Moreover, we were able to correlate the ability of polyLM to induce longer neurites (Fig. 1F and G) with an increased activation of both integrin receptors and the PI3 kinase/AKT signaling pathway.

3.2. LM coating improves DRG neurite outgrowth on PCL filaments

Filaments made of PCL have been previously described as being able to support both neurite extension (in vitro) and axonal growth (in vivo) [26–29]. Thus, here we asked whether PCL filaments covered with LM would provide an improved substrate for DRG neurite outgrowth. First, we assessed PCL filaments by scanning electron microscopy in low and high magnifications (Fig. 2A and B). The integrity of the six microgrooves could be identified in both magnifications. After incubation with either LM or polyLM, filaments were observed using confocal microscopy after immunofluorescence of LM. LM was readily seen as a homogenous coat, whereas differences between the two types of LM were not distinguishable
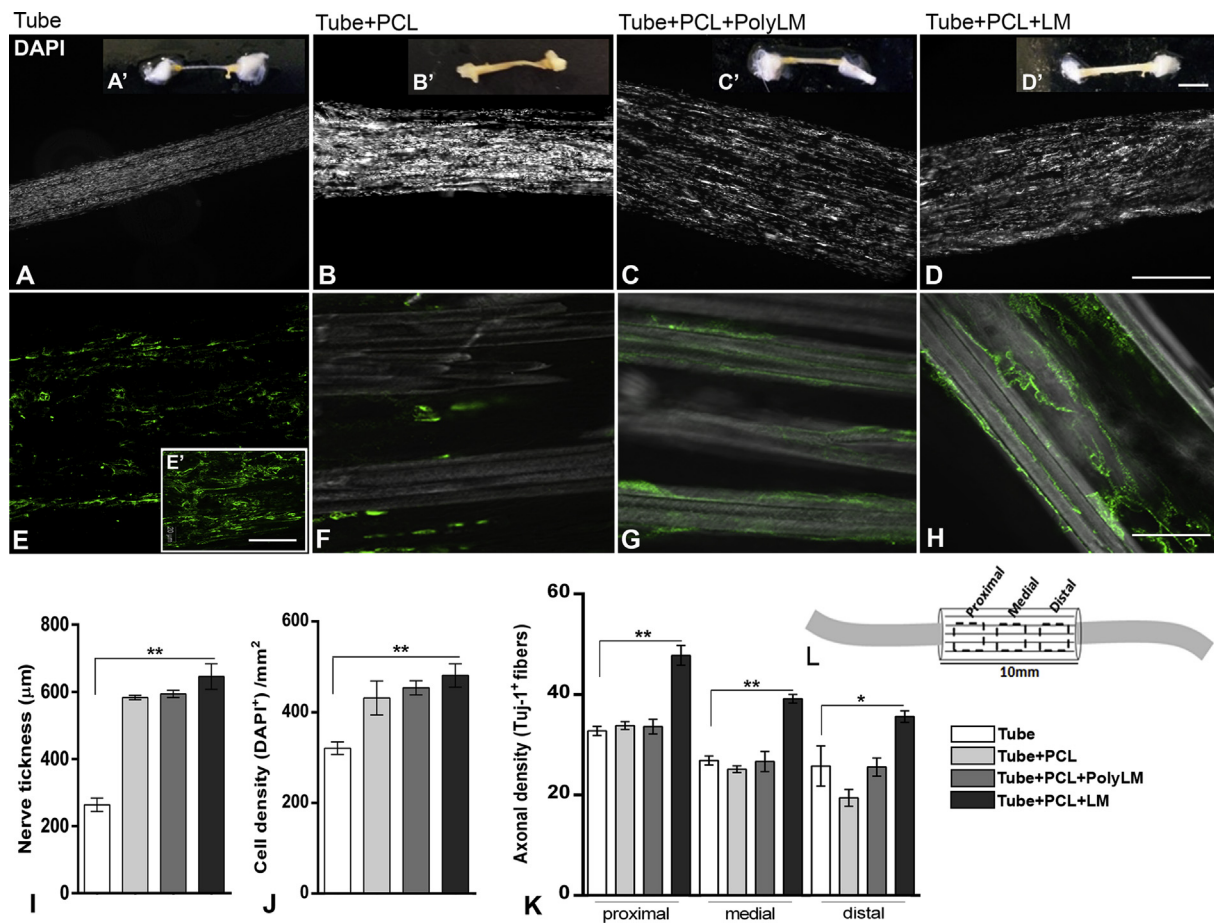
Fig. 3. Microstructured PCL filaments coated with laminin promote sciatic nerve tissue regeneration. Twelve weeks after lesion and insertion of nerve stumps into silicone tubes, regenerated nerves were removed from the tubes and photographed as whole mounts (A'–D') or cut longitudinally for analysis under confocal fluorescence microscopy. (A–D) Sections stained with DAPI; (E–H) optical slices obtained by superimposing differential interference contrast (DIC) and fluorescence of TUJ-1–immunolabeled fibers. The experimental groups were empty tubes (A and E), tubes filed with uncoated PCL filaments (B and F), and PCL filaments precoated with polyLM (C and G) or LM (D and H). The inset E' corresponds to an amplified image of (E) to reveal the unorganized pattern of fiber growth within the empty tube. (I–K) Quantitative analyses or nerve thickness, cell and axonal densities (TUJ-1$^+$ axons) at the experimental conditions described previously. (L) An illustration of the nerve segments, proximal, medial, and distal, shown in (K). Scale bars: (A–D) = 50 μm, (E–H) = 100 μm, (E') = 150 μm. *$p < 0.01$; **$p < 0.001$ by one-way ANOVA. PCL, poly-ε-caprolactone; DAPI, 4′,6-diamidino-2-phenylindole dihydrochloride; ANOVA, analysis of variance; polyLM, polylaminin; LM, laminin.

(Fig. 2C and D). Next, we placed DRG explants on top of the LM precoated filaments and incubated them for 48 h in the presence of NGF. After immunofluorescence for Tuj-1, we found that neurites grew longer distances on either LM-coated filaments than PLO (Fig. 2E–H, ANOVA, *$p < 0.01$*). However, the neurite density was much superior on polyLM than on both PLO and LM (Fig. 2E–G, I). Neurites tended to grow associated with the grooves on the filaments, a feature particularly clear when LM was used in the polymerized form (polyLM) (Fig. 2F, white arrows).

3.3. LM coating of PCL filaments improved regeneration of sciatic nerves in adult rats

The regenerative potential of the LM-coated filaments was tested *in vivo* in a model of sciatic nerve lesion. After surgical removal of 10 mm of the rat sciatic nerve, both proximal and distal stumps were introduced at the edges of a 12-mm silicone tube filled with a bundle of PCL filaments, precoated or not precoated with LM which was previously polymerized (polyLM) or not (LM). Twelve weeks after implantation, we analyzed longitudinal sections of the regenerated sciatic nerve inside the tube either by DAPI staining, to compare nerve thickness and cell density (Fig. 3A–D), or by Tuj-1 immunofluorescence, to evaluate axonal regrowth (Fig. 3E–H). Whole mounts of the regenerated nerves are

shown at the upper part of panels A–D (Fig. 3). It can be appreciated that in 12 weeks, a nerve bridge was formed in all experimental conditions (Fig. 3A'-D'), although the group that received only the silicone tube presented the thinnest nerve among all experimental groups. Uncoated, LM-coated, and polyLM-coated filaments presented similar nerve thicknesses (Fig. 3B–D, I). Cellular densities assessed as the number of DAPI$^+$ cells per mm^2 showed increased cellularity in all groups containing filaments in comparison with the group receiving empty tubes (Fig. 3A–D, J). Axonal regeneration was evaluated by assessing Tuj-1$^+$ fibers. Inside the tube lacking PCL filaments, we often observed clusters of Tuj-1$^+$ axons growing apparently without direction, as demonstrated in Fig. 3E (insert). This suggests that PCL filaments play a role in providing directional axonal guidance towards the distal stump. Such guidance favored the extension of straight axons on plain and polyLM-coated filaments, but resulted in a reticular mesh of axons on the LM group. Quantitative analyses demonstrated that PCL filaments coated with LM presented higher axonal density than the other experimental conditions (Fig. 4 E–H, K). Equivalent results were obtained at proximal, medial, and distal areas of the regenerated nerve. We conclude here that functionalized PCL filaments precovered with LM provided the best environment for nerve tissue replacement among the experimental conditions analyzed.
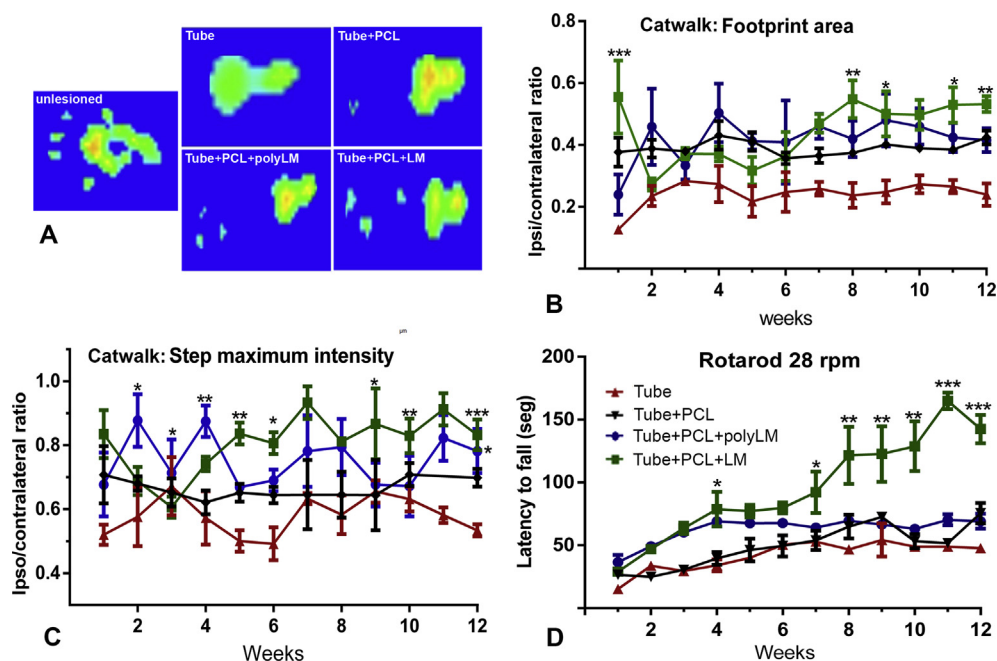
Fig. 4. LM-coated PCL filaments improve motor functional recovery. (A) Representative images of the footprints obtained with the CatWalk system® for the unlesioned animal limb and for the injured limbs of animals in each experimental condition. The intensity of the print is expressed according to the color scale shown in the figure. (B–C) Plots of footprint areas (B) and step maximal intensities (C) against time in weeks after lesion, provided as ratios of the values found for ipsilateral and contralateral paws. (D) Plot of the latency times to fall obtained from the Rotarod® apparatus measured weekly for 12 weeks. Red, black, blue, and green lines represent groups receiving empty tubes, tubes filled with uncoated PCL filaments, tubes filled with polyLM-coated or with LM-coated PCL filaments, respectively. *$p < 0.01$; **$p < 0.001$; ***$p < 0.0001$ by one-way ANOVA. LM, laminin; polyLM, polylaminin; PCL, poly-ε-caprolactone; ANOVA, analysis of variance.

3.4. LM-coated PCL filaments improve motor function in adult rats after sciatic nerve transection

A possible correlation between nerve regeneration and improved locomotor behavior was sought by using a series of motor tests applied throughout the 12 weeks of the experiment. Evaluation of footprints in all experimental conditions, including unlesioned animals, was captured, and we observed that none of the experimental groups was able to completely recover the footprint parameters of the unlesioned group (Fig. 4A). However, animals receiving LM-coated filaments presented the most preserved footprint profile among all groups (Fig. 4A), where the heel and three digits simultaneously contacted the platform. Quantitative analyses detected a significant difference only between LM and empty tube groups at 1, 8, 9, 11, and 12 weeks after the implant (Fig. 4B). We further analyzed the maximum intensity of the step and found statistically significant improvements relative to the empty tube on the polyLM group at 2, 4, and 12 weeks and on the LM group after the fifth week except at 7, 8, and 11 weeks. Animals implanted with uncoated PCL filaments had no significant difference on step maximum intensity compared with the empty tube (Fig. 4C). Finally, we challenged rats over twelve weeks every week on the Rotarod apparatus. The animals were placed on a cylinder rotating at 28 RPM, and we measured the latency time they could remain on the cylinder before falling down. From the seventh week, animals that received LM-coated filaments displayed a consistently higher latency time than those in all the other groups (Fig. 4D). Taken together, the results presented in this setup allowed us to correlate sciatic nerve tissue replacement with better motor functional recovery in rats implanted with the silicone tube filled with LM-coated PCL filaments.

3.5. LM-coated PCL filaments regenerate motor axons functionally

We had previously demonstrated by *in intro* assays that rat sensory DRG explants incubated on polyLM-coated PCL filaments had an extensively neurite outgrowth in distance and in density. This neuritogenesis was significantly better than other experimental conditions. However, by *in vivo* assays and behavioral tests twelve weeks after implantation, it became clear that LM-coated PCL filaments, instead of polyLM-coated ones, provided the best experimental condition for nerve tissue replacement. This observation was in principle unexpected; however,

taking into account that the sciatic nerve is composed of both sensory and motor axons, we considered that LM coating could selectively induce growth of motor fibers over sensitive ones. We thus labeled regenerated nerves simultaneously with ChAT and Tuj-1 to assess the proportion of motor/total axons in each experimental group. We found that although the number of ChAT-positve fibers was higher in the LM-coated group (Fig. 5 A), the proportion of motor relative to total Tuj-1$^+$ fibers exhibited only a slight tendency to higher values on LM-coated PCL filaments (Fig. 5 B). By apotome microscopy, we identified the fluorescence of α-bungarotoxin, which binds to cholinergic receptors on lateral gastrocnemius muscle fibers (Fig. 5C–F). We observed motor end plates in all experimental conditions, but the quantitative analysis demonstrates 2-fold increase in α-bungarotoxin$^+$ events in LM-coated PCL filaments compared with the other experimental conditions (Fig. 5G, ANOVA, $p < 0.001$). These observations led us to conclude that complete axonal regeneration can be attained using LM-coated PCL filaments. In addition, we found indications that the better results observed with the latter conduit were, at least partially, due to the positive effect of the LM-coated filaments on motor axons of the sciatic nerve.

5. Discussion

In this work, we demonstrated that LM-coated PCL filaments efficiently support axonal regeneration across a 10-mm nerve gap twelve weeks after experimental lesion in adult rats. We found that LM, that is, LM diluted to 50 μg/mL in a neutral buffer, a condition in which the protein does not polymerize in solution [30,31], provided a better coating than polyLM. polyLM corresponds to a suspension of self-associated LM molecules of biomimetic properties, readily obtained when LM is diluted down to the same concentration (50 μg/mL) in an acidic buffer [20,31]. Curiously, initial *in vitro* experiments using DRG explants had indicated that polyLM absorbed to either coverslips or PCL filaments supported a higher level of neuritogenesis than LM, which can be explained by the distinct signaling pathways involved in the responses to each substrate. Although the exact signaling cascades triggered by each form of LM have not been fully characterized yet, it has already been described that the response to polyLM requires activation of PKA, while that to LM is independent of PKA and sensitive to inhibitors of ERK1/2 [21,22]. The distinct effects of LM and polyLM *in vitro* versus *in vivo* are probably related to the fact that DRG neurite outgrowth *in vitro* does not
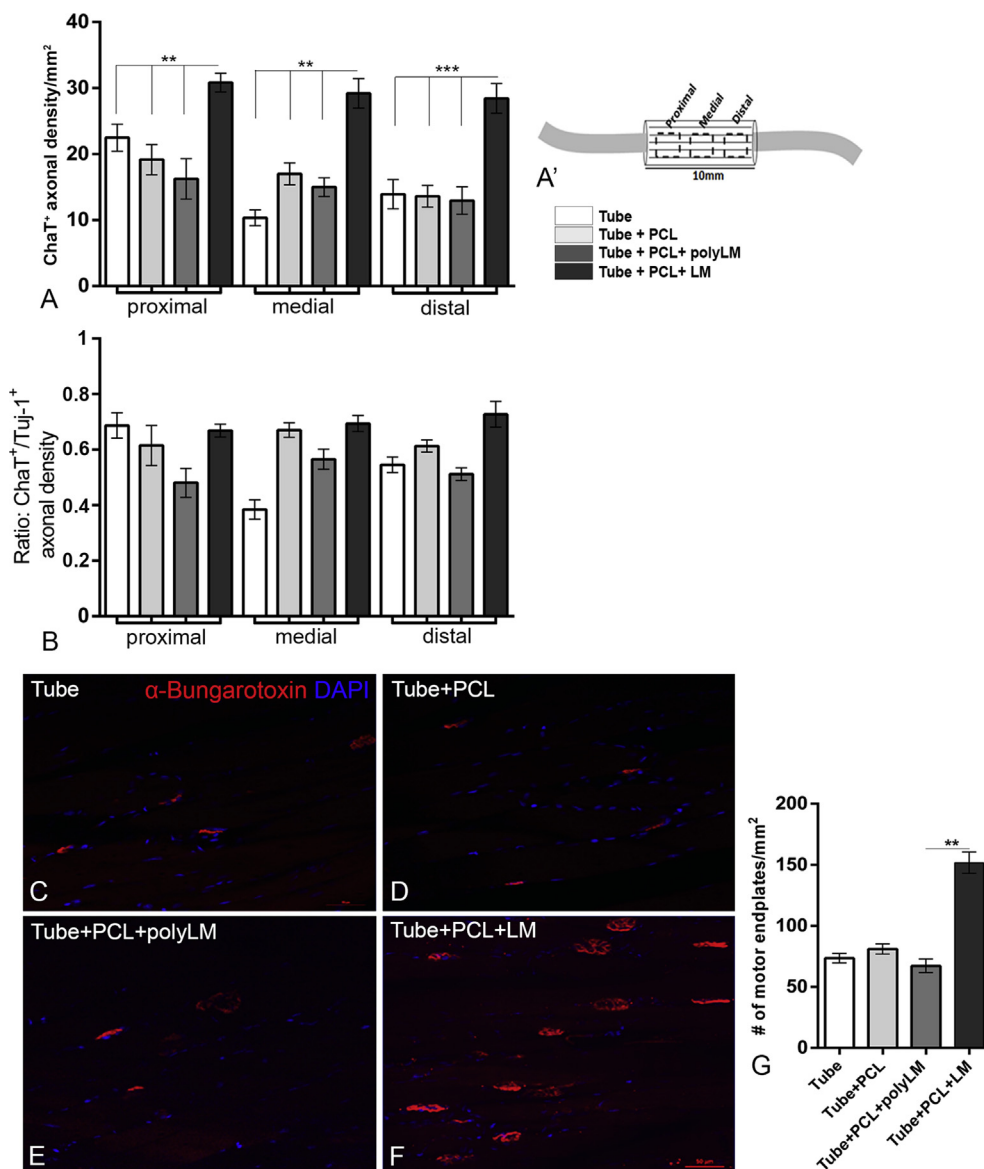
Fig. 5. LM-coated PCL filaments promote motor axon regeneration and muscle reinnervation. (A) Quantitative analysis of fluorescence density of ChAT-positive axons in the regenerated nerve. (A′) An illustration of the nerve segments, proximal, medial, and distal, shown in (A). (B) Ratios of ChAT/Tuj-1–labeled axons on longitudinal sections of the regenerated sciatic nerve tissue twelve weeks after lesion in adult rats. (C–F) Photomicrographs of motor end plates visualized by CY3-conjugated α-bungarotoxin incubated on longitudinal sections of the lateral gastrocnemius muscle. Images were captured by Apotome® microscopy from sections of the following experimental conditions: empty tubes, tubes filled with uncoated PCL filaments, tubes filled with polyLM-coated or with LM-coated PCL filaments. (G) Quantitative analysis of the number of motor end plates per square millimeter. Scale bar: (A–D) = 50 μm. Statistics: **$p < 0.01$; ***$p < 0.001$; $p > 0.05$ by one-way ANOVA. LM, laminin; PCL, poly-ε-caprolactone; ANOVA, analysis of variance; polyLM, polylaminin.

represent exactly a model of regeneration of an injured peripheral nerve. First, DRGs contain only sensory neurons, whereas the sciatic nerve possesses both sensory and motor fibers. We considered that the two forms of the protein could differently affect sensory and motor neurons; the former would respond to polyLM, whereas the latter would respond to LM. Our observation that the proportion of motor fibers relative to total fibers in the regenerated nerves was only slightly increased on LM-coated filaments in comparison with polyLM suggests that this is probably not the only explanation. Nevertheless, the fact that more end plates at the target muscle and superior motor performance occurred in rats of the LM group supports the notion that LM favors motor recovery beyond polyLM. We have observed that only axons extending on LM-coated PCL filaments exhibited a reticular morphology made of branching fibers (Fig. 3). One possibility is that LM induces more branching and this will facilitate the formation of more end plates at the muscle fiber. In this regard, it has been shown that a higher number of collateral fibers during the regenerative process correlate with motor function [32–34].

An alternative explanation is that the axonal growth promoted by polyLM on central axons would require contact with neuronal cell bodies as present in DRGs, but such stimulation would not be effective in the environment of the regenerating sciatic nerve, where the protein is contacted only by the axons. polyLM has been demonstrated to favor neurite/axon extension more efficiently than LM in vitro, using different types of neurons from the central nervous system, including E14 and P2 neurons isolated from the brain cortex [21], retinal cells from newborn animals [22], and embryonic motor neurons isolated from the spinal cord (R.d.S.S. and T.C.-S., unpublished). Moreover, polyLM, but not LM, induced functional axonal regeneration in vivo after spinal cord injury [23]. It is reasonable to conceive that peripheral axons regenerating within the nerve will respond differently to extracellular elements than whole neurons as different receptors can be expressed in growth cones and at the cell soma.

Alternative reasons can explain why polyLM was not more effective than LM in sciatic nerve regeneration. For instance, the environment of nerve injury is less restrictive to the penetration of cells from the immune system and from the surrounding connective tissue that will produce ECM proteins to influence regeneration [5]. Besides, unlike oligodendrocytes, SCs are capable of producing a new basal lamina to support axonal regeneration. Studies are currently being developed to determine whether the LM substrates will distinctly modulate the behavior of these cell types.

It is known that the levels of integrins expressed by neurons during development are reduced in the adult, but they increase again after a peripheral nerve lesion. Immediately after nerve lesion, $\alpha7\beta1$ mRNA increases by 0.4-fold and 1-fold in sensory and motor neurons, respectively, after incubation on the LM substrate. However, motor neurons increase the mRNA levels for the integrin $\alpha5\beta1$ receptor by almost 4-fold, indicating the preference of these cells for fibronectin [30,32]. The differential expression of ECM receptors in distinct neurons at different conditions adds complexity to the system and indicates that further experiments will be necessary to fully understand the contribution of exogenous LM to nerve repair.

One interesting finding of the present study was that using DRG explants only on polyLM, we observed evidence of LM-induced integrin activation beyond the basal level obtained on PLO. It is possible that non-polymerized LM is recognized by other receptors such as dystroglycan or that individual protein units in LM do bind to integrins but do not provoke FAK phosphorylation [35]. Nevertheless, previous studies have shown that the response of DRG neurons to LM involves FAK phosphorylation [36]. One possibility is that LM is already present in the DRG explant, and thus, plating on coverslips coated with LM does not induce further activation of FAK. Moreover, in 7 days of culture, cells within the explant plated on PLO could produce enough LM to account for phosphorylation levels of FAK and AKT similar to those obtained on LM. In any case, our results clearly point to an ability of polyLM to activate integrins in a way that LM does not. This is somehow an expected finding, given that FAK phosphorylation requires approximation of integrin receptors at the plasma membrane. Because polyLM corresponds to an array of LM molecules placed within a fixed distance, one can imagine that polyLM favors the simultaneous engagement of a cluster of integrin receptors. In this regard, it has been reported that the ideal distance between fibronectin-binding motif Arg-Gly-Asp (RGD peptides) to mobilize integrin receptors on fibroblasts is approximately 58 nm [37]. Integrins bind to laminin globular (LG) domains at the distal ends of LM long arms. In polyLM, the distance between contiguous LG domains is predicted to be 52 nm [20], which raises the hypothesis that the specific properties of polyLM can be attributed to its ability to induce clustering of integrin receptors, increasing FAK activation.

The biomaterial sciences and the consequent variety of strategies for tissue engineering of peripheral nerves have increased exponentially over the last twenty years. The results clearly demonstrate the potential of biocompatible materials to efficiently modulate the immune system, SCs, connective tissue cells, as well as peripheral and central neurons to promote regenerative processes. The frequency of drawbacks due to immune response against the implants has decreased as much as technologies to produce new biomaterials are refined. A standard material such as chitosan, for instance, is being gradually replaced by PCL, pure or combined, over other polymers, which has provided increasingly higher efficiency [26,27]. One of the big issues at this moment is how complex and expensive the biomaterial production has become, many times showing promising results on nerve tissue replacement but requiring costs beyond the translational reality. Moreover, clinical validation of new materials in translational medicine requires extensive toxicity studies in different animal models to support their expected safety in future human trials. Accordingly, ethics committees devoted to regulating human research tend to privilege the use of molecules that have already been previously demonstrated safe for animals and humans. All these aspects considered, we believe that the graft composed of a silicone tube filled with LM-coated microstructured PCL filaments, shown in this work to promote massive nerve tissue replacement with a good balance among total cell density, axonal regeneration, and functional recovery, emerges as a simple, unexpansive, and efficient candidate for a future clinical trial for nerve repair. The fact that both PCL and LM have already been used in other animals besides rodents, as well as in humans in the past, further supports this notion [38,39]. Finally, it is important to mention that although experimental models of nerve regeneration normally focus on restoring tissue damage provoked by traumatic injury, owing to easiness of reproducing such lesions in standardized studies, in the clinical scenario, nerve repair strategies are often needed to treat other nerve injuries such as a compressive lesion due to tumor growth and disease-associated losses such as those observed in leprosy, which broadens the need for developing new treatments.

Data statement

The raw/processed data required to reproduce these findings cannot be shared at this time as the data also form part of an ongoing study.

Conflict of interest

The authors declare no conflict of interest in this manuscript.

References

[1] Z.L. Chen, W.M. Yu, S. Strickland, Peripheral regeneration, Annu. Rev. Neurosci. 30 (2007) 209–233. https://doi.org/10.1146/annurev.neuro.30.051606.094337.

[2] H.J. Weinberg, P.S. Spencer, The fate of Schwann cells isolated from axonal contact, J. Neurocytol. 7 (1978) 555–569. https://doi.org/10.1007/BF01260889.

[3] M.D. Ard, R.P. Bunge, M.B. Bunge, Comparison of the Schwann cell surface and Schwann cell extracellular matrix as promoters of neurite growth, J. Neurocytol. 16 (1987) 539–555. https://doi.org/10.1007/BF01668507.

[4] W. Tetzlaff, Tight junction contact events and temporary gap junctions in the sciatic nerve fibres of the chicken during Wallerian degeneration and subsequent regeneration, J. Neurocytol. 11 (1982), 83 -58, https://doi.org/10.1007/BF01153522.

[5] M.E. Vargas, B.A. Barres, Why is Wallerian degeneration in the CNS so slow? Annu. Rev. Neurosci. 30 (2007) 153–179. https://doi.org/10.1146/annurev.neuro.30.051606.094354.

[6] A. Bignami, N.H. Chi, D. Dahl, Laminin in rat sciatic nerve undergoing Wallerian degeneration. Immunofluorescence study with laminin and neurofilament antisera, J. Neuropathol. Exp. Neurol. 43 (1984) 94–103. https://doi.org/10.1097/00005072-198401000-00008.

[7] F.M. Longo, E.G. Hayman, G.E. Davis, E. Ruoslahti, E. Engvall, M. Manthorpe, S. Varon, Neurite-promoting factors and extracellular matrix components accumulating in vivo within nerve regeneration chambers, Brain Res. 309 (1984) 105–117. https://doi.org/10.1016/0006-8993(84)91014-X.

[8] A. Tona, G. Perides, F. Rahemtulla, D.J. Dahl, Extracellular matrix in regenerating rat sciatic nerve: a comparative study on the localization of laminin, hyaluronic acid, and chondroitin sulfate proteoglycans, including versican, Histochem Cytochem 41 (1993) 593–599. https://doi.org/10.1177/41.4.8450198.

[9] S.L. Palm, L.T. Furcht, Production of laminin and fibronectin by Schwannoma cells: cell-protein interactions in vitro and protein localization in peripheral nerve in vivo, J. Cell Biol. 96 (1983) 1218–1226. http://doi.org/10.1083/jcb.96.5.1218.

[10] M. Manthorpe, E. Engvall, E. Ruoslahti, F.M. Longo, G.E. Davis, S. Varon, Laminin promotes neuritic regeneration from cultured peripheral and central neurons, J. Cell Biol. 97 (1983) 1882–1890. http://doi.org/10.1083/jcb.97.6.1882.

[11] G.E. Davis, M. Manthorpe, E. Engvall, S. Varon, Isolation and characterization of rat schwannoma neurite-promoting factor: evidence that the factor contains laminin, J. Neurosci. 5 (1985) 2662–2671. https://doi.org/10.1523/JNEUROSCI.05-10-02662.1985.

[12] D.M. Barnes, What makes nerves regenerate? Science 230 (1985) 1024–1025. https://doi.org/10.1126/science.4059920.

[13] B.S. Weeks, B. Papadopoulos, M. Dym, H.K. Kleinman, cAMP promotes branching of laminin-induced neuronal processes, J. Cell. Physiol. 147 (1991) 62–67. https://doi.org/10.1002/jcp.1041470109.

[14] Q. Chen, M.S. Kinch, T.H. Lin, K. Burridge, R.L. Juliano, Integrin-mediated cell adhesion activates mitogen-activated protein kinases, J. Biol. Chem. 269 (1994) 26602–26605.

[15] D.S. Gary, M.P. Mattson, Integrin signaling via the PI3-kinase-Akt pathway increases neuronal resistance to glutamate-induced apoptosis, J. Neurochem. 76 (2001) 1485–1496. https://doi.org/10.1046/j.1471-4159.2001.00173.x.

[16] J.P. Myers, E. Robles, A. Ducharme-Smith, T.M. Gomez, Focal adhesion kinase modulates Cdc42 activity downstream of positive and negative axon guidance cues, J. Cell Sci. 125 (2012) 2918–2929. https://doi.org/10.1242/jcs.100107.

[17] J.P. Myers, T.M. Gomez, Focal adhesion kinase promotes integrin adhesion dynamics necessary for chemotropic turning of nerve growth cones, J. Neurosci. 31 (2011) 13585–13595. https://doi.org/10.1523/JNEUROSCI.2381-11.2011.

[18] E. Hohenester, P.D. Yurchenco, Laminins in basement membrane assembly, Cell Adhes. Migrat. 7 (2013) 56–63. https://doi.org/10.4161/cam.21831.

[19] P.D. Yurchenco, Y.S. Cheng, H. Colognato, Laminin forms an independent network in basement membranes, J. Cell Biol. 117 (1992) 1119–1133. http://doi.org/10.1083/jcb.117.5.1119.

[20] M.M. Barroso, E. Freire, G.S. Limaverde, G.M. Rocha, E.J. Batista, G. Weissmüller, L.R. Andrade, T. Coelho-Sampaio, Artificial laminin polymers assembled in acidic pH mimic basement membrane organization, J. Biol. Chem. 283 (2008) 11714–11720. https://doi.org/10.1074/jbc.M709301200.

[21] E. Freire, F.C. Gomes, R. Linden, V.M. Neto, T. Coelho-Sampaio, Structure of laminin substrate modulates cellular signaling for neuritogenesis, J. Cell Sci. 115 (2002) 4867–4876. https://doi.org/10.1242/jcs.00173.

[22] C. Hochman-Mendez, J.R. Lacerda de Menezes, A. Sholl-Franco, T. Coelho-Sampaio, Polylaminin recognition by retinal cells, J. Neurosci. Res. 92 (2014) 24–34. https://doi.org/10.1002/jnr.23298.

[23] K. Menezes, J.R. de Menezes, M.A. Nascimento, R. de S. Santos, T. Coelho-Sampaio, Polylaminin, a polymeric form of laminin, promotes regeneration after spinal cord injury, FASEB J. 24 (2010) 4513–4522. https://doi.org/10.1096/fj.10-157628.

[24] D. Angius, H. Wang, R.J. Spinner, Y. Gutierrez-Cotto, M.J. Yaszemski, A.J. Windebank, A systematic review of animal models used to study nerve regeneration in tissue-engineered scaffolds, Biomaterials 33 (2012) 8034–8039. https://doi.org/10.1016/j.biomaterials.2012.07.056.

[25] X. Jiang, S.H. Lim, H.Q. Mao, S.Y. Chew, Current applications and future perspectives of artificial nerve conduits, Exp. Neurol. 223 (2010) 86–101. https://doi.org/10.1016/j.expneurol.2009.09.009.

[26] T.K. Dash, V.B. Konkimalla, Poly-ε-caprolactone based formulations for drug delivery and tissue engineering: a review, J. Control. Release 158 (2012) 15–33. https://doi.org/10.1016/j.jconrel.2011.09.064.

[27] V. Chiono, G. Vozzi, F. Vozzi, C. Salvadori, F. Dini, F. Carlucci, M. Arispici, S. Burchielli, F. Di Scipio, S. Geuna, M. Fornaro, P. Tos, S. Nicolino, C. Audisio, I. Perroteau, A. Chiaravalloti, C. Domenici, P. Giusti, G. Ciardelli, Melt-extruded guides for peripheral nerve regeneration. Part I: poly(ε-caprolactone), Biomed. Microdevices 11 (2009) 1037–1050. https://doi.org/10.1007/s10544-009-9321-9.

[28] M. Labet, W. Thielemans, Synthesis of polycaprolactone: a review, Chem. Soc. Rev. 38 (2009) 3484–3504. https://doi.org/10.1039/b820162p.

[29] V.T. Ribeiro-Resende, B. Koenig, S. Nichterwitz, S. Oberhoffner, B. Schlosshauer, Strategies for inducing the formation of bands of Büngner in peripheral nerve regeneration, Biomaterials 30 (2009) 5251–5259. https://doi.org/10.1016/j.biomaterials.2009.07.007.

[30] P.D. Yurchenco, E.C. Tsilibary, A.S. Charonis, H. Furthmayr, Laminin polymerization in vitro. Evidence for a two-step assembly with domain specificity, J. Biol. Chem. 260 (1985) 7636–7644.

[31] E. Freire, T. Coelho-Sampaio, Self-assembly of laminin induced by acidic pH, J. Biol. Chem. 275 (2000) 817–822. https://doi.org/10.1074/jbc.275.2.817.

[32] F. Gonzalez-Perez, A. Alé, D. Santos, C. Barwig, T. Freier, X. Navarro, Udina E Substratum preferences of motor and sensory neurons in postnatal and adult rats, Eur. J. Neurosci. 43 (2015) 431–442. https://doi.org/10.1111/ejn.13057.

[33] B.G. Jiang, X.F. Yin, D.Y. Zhang, Z.G. Fu, H.B. Zhang, Maximum number of collaterals developed by one axon during peripheral nerve regeneration and the influence of that number on reinnervation effects, Eur. Neurol. 58 (2007) 12–20. https://doi.org/10.1159/000102161.

[34] N. Lago, X. Navarro, Correlation between target reinnervation and distribution of motor axons in the injured rat sciatic nerve, J. Neurotrauma 23 (2006) 227–240. https://doi.org/10.1089/neu.2006.23.227.

[35] I. Ivankovic-Dikic, E. Grönroos, A. Blaukat, B.U. Barth, I. Dikic, Pyk2 and FAK regulate neurite outgrowth induced by growth factors and integrins, Nat. Cell Biol. 2 (2000) 574–581. https://doi.org/10.1038/35023515.

[36] B.A. Tucker, M. Rahimtula, K.M. Mearow, Src and FAK are key early signalling intermediates required for neurite growth in NGF-responsive adult DRG neurons, Cell. Signal. 20 (1) (2008) 241–257. https://doi.org/10.1016/j.cellsig.2007.10.014.

[37] E.A. Cavalcanti-Adam, A. Micoulet, J. Blümmel, J. Auernheimer, H. Kessler, J.P. Spatz, Lateral spacing of integrin ligands influences cell spreading and focal adhesion assembly, Eur. J. Cell Biol. 85 (2006) 219–224. https://doi.org/10.1016/j.ejcb.2005.09.011.

[38] R.A. Neal, S.M. Lenz, T. Wang, D. Abebayehu, B.P. Brooks, R.C. Ogle, E.A. Botchwey, Laminin- and basement membrane-polycaprolactone blend nanofibers as a scaffold for regenerative medicine, Nanomater Environ 2 (2014) 1–12. https://doi.org/10.2478/nanome-2014-0001.

[39] A. Carrier-Ruiz, F. Evaristo-Mendonça, R. Mendez-Otero, V.T. Ribeiro-Resende, Biological behavior of mesenchymal stem cells on poly-ε-caprolactone filaments and a strategy for tissue engineering of segments of the peripheral nerves, Stem Cell Res. Ther. 6 (2015) 128. http://doi.org/10.1186/s13287-015-0121-2.